

Influence of the relative rate of reaction and transport process on the micro- and macrostructure of precipitation reaction products

Theses of doctoral (PhD) dissertation

Edina Papp-Balog

Supervisor: Dr. Gábor Schuszter, *assistant professor*

Doctoral School of Chemistry

University of Szeged, Department of Physical Chemistry and Materials
Science

2024

1 Introduction and Aim

Precipitation reactions are abundant in our environment, for example, they play a vital role in the formation of various minerals that are present in Nature, and similarly in industrial applications (e.g., wastewater and gas purification, synthesis of pigments). Furthermore, these reactions are also significant in the field of research, since they enable the detection of different ions, which can be used for qualitative and quantitative analysis as well. In addition, by using precipitation reactions, we can synthesize products for further applications (e.g., pharmaceutically relevant polymorphs, catalytically active materials). Due to this, it is very important to develop appropriate synthesis methods. Traditionally, solid products are produced in a well-stirred system in which the reactants are mixed. However, there are many examples in the literature where precipitates have been synthesized in systems far from equilibrium. When the precipitation reactions are coupled to various transport phenomena (e.g., flow, diffusion), different spatial gradients can evolve, which can be externally controlled by changing the experimental parameters. Therefore, we can achieve improved control over product properties (micro- and macrostructure), which proves the advantage of far-from-equilibrium systems over well-stirred methods. Based on these, by using techniques coupled to transport processes, we can also synthesize products which would not be available in a well-stirred system (e.g., thermodynamically less stable polymorphs). A possible application of these synthesis methods is the production of zeolitic imidazolate framework (ZIF) crystals, which have recently gained a great interest in the literature. The reaction of zinc(ZIF-8) and cobalt(ZIF-67) ions with 2-methyl-imidazole (2-MeIm) can lead to the formation of different polymorphs depending on the applied experimental conditions. The sodalite-type polymorphs possess porous structure, and thus a huge specific surface area, but their formation is thermodynamically less favored compared to other polymorphs. Therefore, it is important to develop an optimized synthesis method that enables the production of the thermodynamically less stable polymorphs, and thus the wide spread application of these products (e.g., adsorption of various gases, heterogeneous catalysis).

During my doctoral studies our aim was to develop a synthesis method in a confined flow reactor which enables the production of ZIF crystals. At first we had to understand the effect of the different experimental parameters on the forming precipitate patterns. Therefore, we have studied the connections between the micro- and macrostructure of the precipitates, and the impact of the reaction rate on the formation of patterns in case of various chemical systems. We have also examined the effect of combined ions on the properties of the evolving patterns and crystals. To produce the desired ZIF crystals in the flow-driven reactor, it has also been essential to explore the kinetics of the nucleation and crystal growth processes. By coupling the typical time scales of precipitation reaction and flow, we have been able to synthesize the different polymorphs of ZIF crystals in a flow-driven system.

2 Experimental Section

During my PhD work, at first the effect of the experimental parameters (e.g., reactant concentrations, flow rate etc.) on the macroscopic precipitate pattern formation was investigated in a confined flow reactor. The correlations between the micro- and macrostructure of the patterns were studied in the case of different precipitates which contained calcium(II) ions, while the impact of the reaction rate was examined by producing various alkaline earth and transition metal oxalate patterns. In the next step we attempted to modify the macrostructure of alkaline earth metal–carbonate precipitate patterns by combining different metal ions. The flow-driven experiments were carried out in a horizontal Hele-Shaw cell shown in Fig. 1a. The experimental setup consisted of a large lower pool ($35\text{ cm} \times 35\text{ cm}$) and a smaller upper plate ($21\text{ cm} \times 21\text{ cm}$) made of Plexiglas, which were placed on a stand. The constant layer thickness ($\sim 0.5\text{ mm}$) between the two Plexiglas plates was ensured by four spacers and four weights, which were placed at the four corners of the cover plate. During the experiments, the thin horizontal gap was first filled with one of the reactant solutions (**A**). To ensure the homogeneous outflow of this solution, the same reactant solution was poured into the pool around the cover plate, thus forming a $\sim 4\text{ mm}$ thick liquid layer. Thereafter, the other reactant solution (**B**) was injected into this through a $\sim 1\text{ mm}$ diameter inlet from the middle of the lower pool by using a syringe pump at different flow rates (Q). The volume (V) of the injected solution was 5 ml in each case. The obtained macroscopic precipitate patterns were recorded from above by a monochrome digital camera. The microstructure of the patterns was investigated by *in situ* optical microscopy if sufficiently large crystals formed during the reactions. However, when the patterns consisted of tiny crystals, it was necessary to take samples from the gap of the reactor for further micro-analysis (e.g., scanning electron microscopy (SEM) and energy dispersive X-ray spectroscopy (EDX)). Therefore, we designed an other upper plate with tiny, systematically positioned and airtight openings on it (top left of Fig. 1a), which enabled the precise sampling and localized examination of the microstructure.

In order to carry out the flow-driven synthesis of ZIF crystals, at first the kinetics of nucleation and crystal growth processes were characterized. The nucleation kinetics was followed by

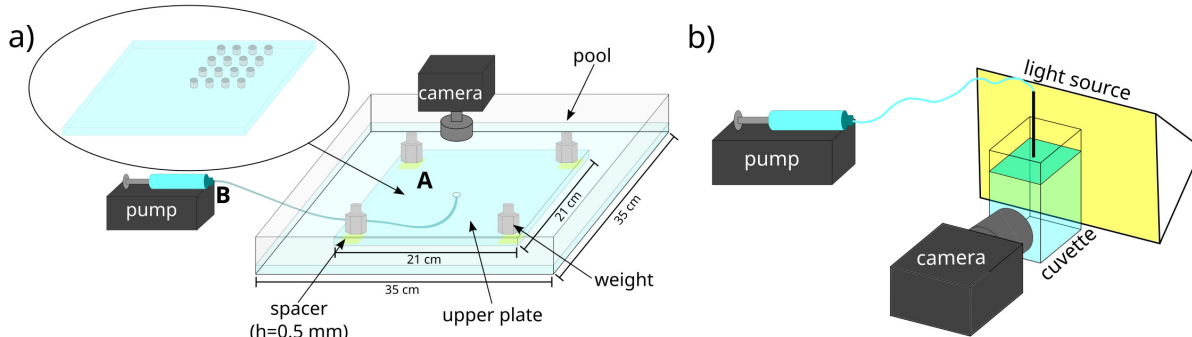


Figure 1: Schematics of the experimental setups used during a) flow-driven synthesis and b) kinetic measurements (high-speed camera).

a high-speed camera method, while the crystal growth was studied with a UV-vis spectrophotometer. In the latter case, the reactants were poured into a cuvette, and the turbidity was measured over time during continuous mixing. The microstructure of the products obtained from the well-stirred system was investigated by various methods (SEM, X-ray diffraction (XRD), Raman and Fourier-transform infrared spectroscopy (FTIR), and N₂ adsorption (BET)). In case of the high-speed camera method, one of the reactant solutions was poured into a cuvette, then the other one was injected into this from above by applying a syringe pump. The mixing of the reactant solutions and the formation of colloidal intermediate were recorded by high-speed camera (Fig. 1b). Based on the images, which were taken during these experiments, the kinetics of the nucleation was characterized by the induction period.

3 New Scientific Results

- I. In case of precipitation reactions, which take place in a confined flow reactor, a precipitate tube structure can evolve due to a phenomenon analogous to viscous fingering, if the nucleation dominates over crystal growth process [4].

The effect of microstructure on macroscopic precipitate pattern formation was studied in the case of calcium phosphate, sulfate, carbonate, and silicate precipitates, which were produced by injecting the solution containing the precipitating anion into a calcium chloride solution. Depending on the chemical nature of the reactants, significantly different precipitate structures formed under the same experimental parameters. While the calcium phosphate and sulfate patterns are characterized by radial symmetry (top panels of Fig. 2a and b), the calcium carbonate and silicate precipitates show membrane-like structures (top panels of Fig. 2c and d). This difference can be explained by the microstructure of the crystals which build up the patterns. In the case of calcium phosphate and sulfate, large particles with low particle density form as a result of the reactions, thus they can sediment earlier during the flow (lower panels of Fig. 2a and b). Hence, the characteristics of the patterns are controlled by the permeability decrease in the reaction gap. In contrast, in the calcium carbonate and silicate systems, a large number of tiny particles appear after the contact of the reactant solutions (lower panels of Fig. 2c and d). Between these small crystals, a van der Waals type interaction can occur which results in a colloidal gel region at the interface between the reactant solutions. Due to this, the viscosity locally increases in the confinement, which generates a viscosity gradient in the system, thus a phenomenon analogous to viscous fingering causes the formation of precipitate membrane structures. According to these results, if the nucleation is the dominant process during precipitate formation, the interaction between the chemical reaction and hydrodynamics is enhanced.

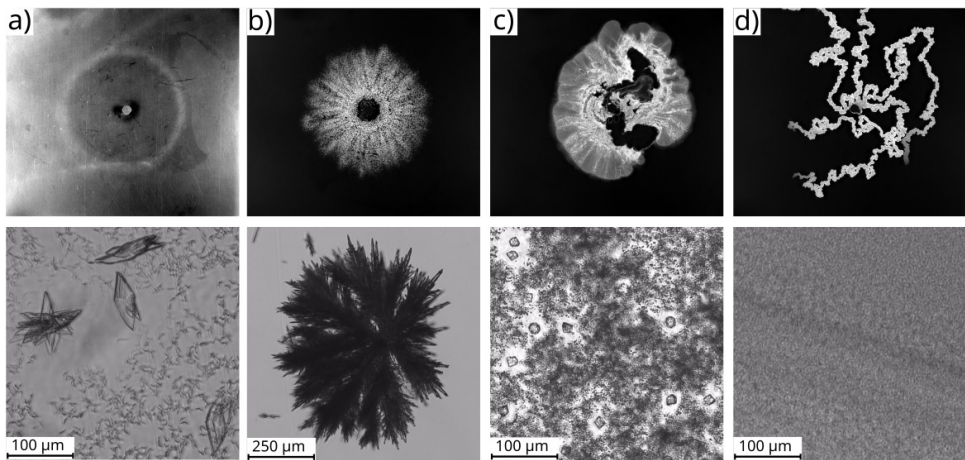


Figure 2: Top panel: Macroscopic a) calcium phosphate, b) sulfate, c) carbonate and d) silicate precipitate patterns obtained during flow-driven experiments; $c_{CaCl_2} = 2 \text{ M}$, $c_{anions} = 1 \text{ M}$, $V = 5 \text{ ml}$. Lower panel: *In situ* optical microscope images of the different crystals taken after the end of injection; $c_{CaCl_2} = 1 \text{ M}$, $c_{anions} = 0.5 \text{ M}$, $V = 3 \text{ ml}$. $Q = 1 \text{ ml/min}$.

II. In case of precipitation reactions, which take place in a confined flow reactor, the ratio between the typical time scales of reaction and flow determines the characteristics of emerging patterns: a relatively slow reaction leads to radial symmetry, while a relatively fast reaction results in complex precipitate pattern [3].

The impact of reaction rate on the macroscopic precipitate pattern formation was investigated in case of various alkaline earth ($Mg(II)$, $Ca(II)$, $Sr(II)$, $Ba(II)$) and transition metal ($Co(II)$, $Ni(II)$, $Cu(II)$, $Zn(II)$) oxalate precipitates, since the kinetics of these reactions had already been known from the literature. During the experiments, the solutions of different precipitating metal ions were filled in between two Plexiglas plates, and then the oxalate solution was injected into them. In case of copper(II) oxalate pattern, which is shown in Fig. 3b, reverse injection was applied. Due to the diverse reaction rates, significantly different precipitate structures form under the same experimental conditions. If the reaction is slow compared to the time scale of flow, the precipitate occurs only later after the contact of the reactant solutions. In this case, the patterns exhibit an annular structure, whose characteristics are only determined by the hydrodynamic instability caused by the density difference between the solutions (close-up in Fig. 3a, appearance of precipitate stripes at the periphery of the pattern). In contrast, if the typical time scales of precipitation reaction and flow are comparable, the crystals appear almost immediately after the contact of the reactant solutions. This results in radially expanding patterns, which also exhibit the characteristics of the flow field (close-up in Fig. 3b, presence of precipitate stripes throughout the pattern). Finally, if the reaction is significantly faster than the flow, a great number of precipitate particles forms, which causes a large interaction between precipitation and hydrodynamics. Due to this, complex precipitate patterns evolve (Fig. 3c, broken radial symmetry).

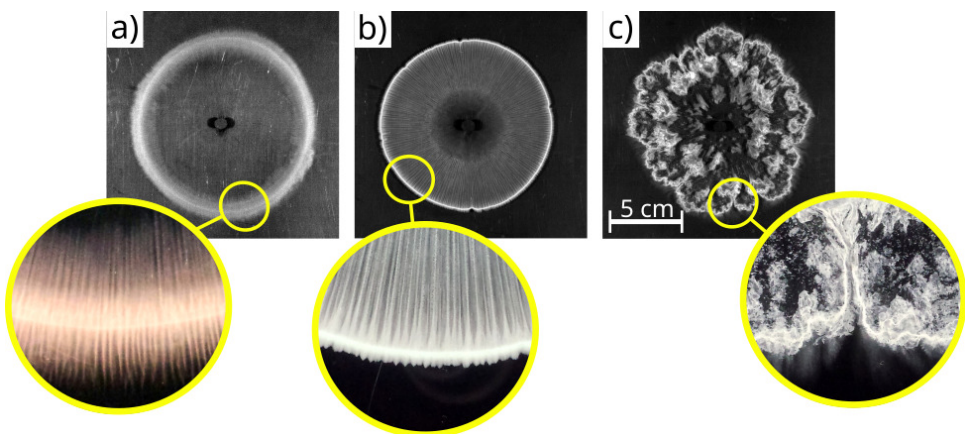


Figure 3: Macroscopic a) cobalt, b) copper and c) calcium oxalate precipitate patterns obtained during flow-driven experiments; $c_{M^{2+}} = c_{(COO)_2^{2-}} = 0.25\text{ M}$, $V = 5\text{ ml}$, $Q = 5\text{ ml/min}$. Close-ups illustrate the periphery of patterns.

III. In case of alkaline earth metal–carbonate precipitation reactions, which take place in a confined flow reactor, the combination of different metal ions can lead to the formation of precipitate tube structures even if the reaction is relatively slow, whose driving force is the promoted nucleation process [1].

The effect of combining ions on the macrostructure of precipitate patterns was examined in case of various alkaline earth metal–carbonate systems. During the reference experiments, the solutions of precipitating metal ions were filled separately in the thin horizontal gap, and then the solution of sodium carbonate was injected into them. At appropriately high reactant concentrations (1.5 M), calcium, strontium, and barium carbonate patterns exhibit a membrane/precipitate tube structure (yellow-marked parts of Fig. 4a). Under these conditions, the supersaturation is high and the nucleation is the beneficiary process. However, in the case of magnesium carbonate, the membrane structure does not evolve at the same experimental parameters, since this reaction is significantly slower as compared to the other systems. Therefore, as a next step, we attempted to modify the characteristics of this pattern by filling a concentrated (1.5 M) magnesium-chloride solution doped with various alkaline earth metal ions in between the Plexiglas plates. This condition can favor the nucleation process and increase the degree of supersaturation. By combining the ions, the characteristics of the magnesium carbonate pattern were successfully modified, and relatively low added alkaline earth metal ion concentration (0.5 M) was already enough to produce the tube-like structures (yellow-marked parts of Fig. 4b). In case of magnesium-free systems we had to use higher concentrations to achieve the membrane structure. Accordingly, the composite system can be characterized by the fastest nucleation among the investigated systems, which suggests that the magnesium and the other alkaline earth metal ions build up together the precipitate tubes.

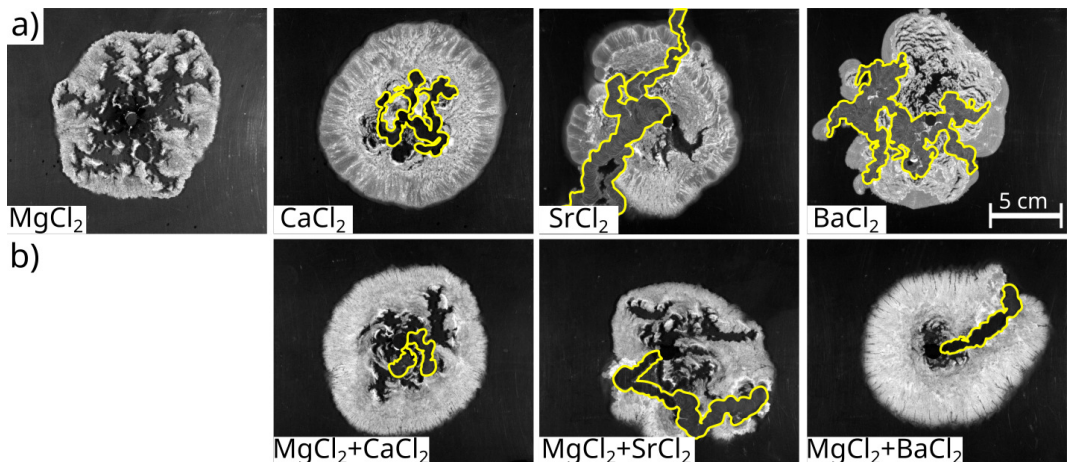


Figure 4: Macroscopic alkaline earth metal carbonate precipitate patterns, when the metal ions were applied a) separately ($c_{M^{2+}} = c_{CO_3^{2-}} = 1.5 \text{ M}$), and b) combined ($c_{Mg^{2+}} = c_{CO_3^{2-}} = 1.5 \text{ M}$, $c_{M^{2+}} = 0.5 \text{ M}$). $V = 5 \text{ ml}$, $Q = 1 \text{ ml/min}$. The yellow-marked parts highlight the precipitate membrane/tube structures within the patterns.

IV. During the aqueous synthesis of zeolitic imidazolate frameworks (ZIF-8, ZIF-67), we can achieve kinetic control over product properties by varying the reactant concentrations: low concentrations and hence slow reactions favor the formation of thermodynamically stable products, while concentrated solutions and thus fast reactions facilitate the production of useful, but thermodynamically less stable polymorphs [2].

During the kinetic characterization of the formation of ZIF-8 type metal–organic frameworks, the aqueous solutions of zinc(II) chloride and 2-MeIm organic ligand were filled into a cuvette, then the turbidity was measured over time by a UV–vis spectrophotometer during constant mixing. In the experiments, the initial concentrations of the reactants were varied at constant stoichiometric ratio. In case of high reactant concentrations and hence fast reactions, the turbidity of the mixture does not change or only slightly vary over time (curves from **I.** to **IV.** in Fig. 5a). In contrast, if we apply lower concentrations, the reactions are slower resulting in a stepwise kinetic curve (curves from **V.** to **VII.** in Fig. 5a), indicating the change of crystal properties during reaction. In order to prove this, the time evolution of crystal morphology (SEM) was investigated in case of two such solution compositions, which resulted in different kinetic curves. It is found that the second turbid-

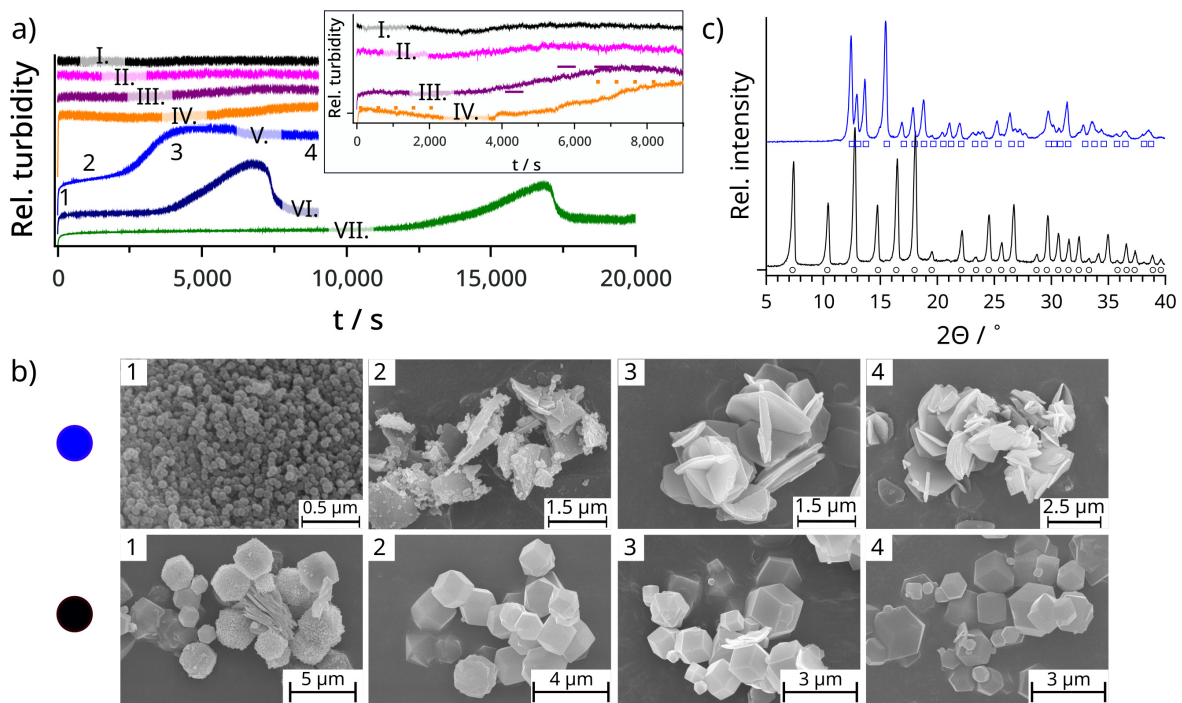


Figure 5: a) Relative turbidity – time curves regarding the formation of ZIF-8 crystals at different solution compositions; $[2\text{-MeIm}]_{\text{tot}}$ and $[\text{Zn}]_{\text{tot}}$: **I.** – 500 and 25 mM, **II.** – 375 and 18.75 mM, **III.** – 250 and 12.5 mM, **IV.** – 160 and 8 mM, **V.** – 80 and 4 mM, **VI.** – 40 and 2 mM, and **VII.** – 30 and 1.5 mM. b) Time evolution of crystal morphology in case of slow (● stepwise turbidity, curve **V.**) and fast (● unchanged turbidity, curve **I.**) reactions. c) Crystalline phase of the final product in case of slow (blue, curve **V.**) and fast (black, curve **I.**) reactions; the blue squares and black circles below the diffractograms belong to the characteristic X-ray diffractions of different polymorphs.

ity increase is indeed related to the recrystallization of the initially formed nanoparticles (top panel of Fig. 5b). However, in the case of constant turbidity, the crystal morphology does not change during the reaction, thus the final product is present from the beginning of the reaction (lower panel of Fig. 5b). In addition, PXRD measurements reveal that in the case of lower concentrations, hence slow reactions the final product is the thermodynamically stable but less useful polymorph. Contrary to this, the higher concentrations, thus fast reactions allow the formation of the less stable but high-porosity polymorph (Fig. 5c). According to these results, the different polymorphs of ZIF-8 can be produced in a well-stirred system via kinetic control. These observations are valid for the ZIF-67 system as well (reaction of cobalt(II) ions with 2-MeIm).

V. *The synthesis of ZIF-8 and ZIF-67 crystals in a flow-driven system and confined reactor enables the coexistent formation of various polymorphs, which are spatially separated.*

The flow-driven synthesis of the ZIF-8 and ZIF-67 types of metal–organic frameworks was carried out by injecting the aqueous solution of 2-MeIm into zinc(II) or cobalt(II) ion solutions, which were pre-filled into the thin horizontal gap. The microstructure of the forming radially symmetric precipitate patterns was investigated by SEM at different distances from the inlet location (numbers in Fig. 6. indicate the place of sampling). In case of ZIF-8 system, it is found that the morphology of the crystals changes along to the radius, which is caused by the modified flow conditions due to the reactor geometry. Close to the inlet, the thermodynamically less stable but useful polymorph forms (Fig. 6a, sampling locations 1., 2. and 3.), while at the periphery of the pattern the more stable polymorph with smaller pore size is present (Fig. 6a, sampling location 4.). The same tendency can be observed in case of ZIF-67 system as shown in Fig. 6b. According to these results, the applied reactor enables the independent removal of the different polymorphs, which supports the advantage of flow-driven synthesis over a well-stirred system.

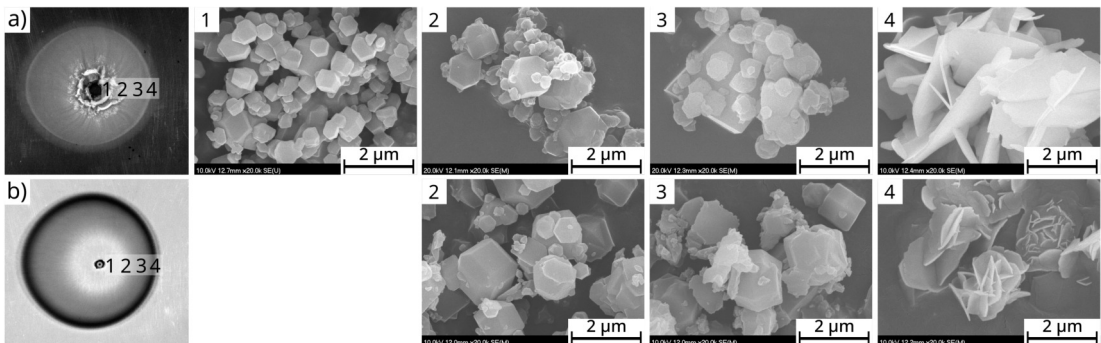


Figure 6: Macrostructure of a) ZIF-8, and b) ZIF-67 precipitate patterns and the morphology of the crystals at different distances from the inlet location. The numbers indicate the place of sampling. $c_{Zn^{2+}} = c_{Co^{2+}} = 0.05 \text{ M}$, $c_{2-MeIm} = 1 \text{ M}$, $V = 5 \text{ ml}$, $Q = 0.5 \text{ ml/min}$.

4 List of Scientific Publications

4.1 Scientific Publications Related to the Dissertation

1. K. Bene, E. Balog, G. Schuszter

Synthesis and composition modification of precipitate tubes in a confined flow reactor

Phys. Chem. Chem. Phys., **25**, 27293 (2023), IF₂₀₂₃ = 2.9

2. E. Balog, G. Varga, Á. Kukovecz, Á. Tóth, D. Horváth, I. Lagzi, G. Schuszter

Polymorph selection of zeolitic imidazolate frameworks via kinetic and thermodynamic control

Cryst. Growth Des., **22**, 4268–4276 (2022), IF₂₀₂₂ = 3.8

3. E. Balog, P. Papp, Á. Tóth, D. Horváth, G. Schuszter

The impact of reaction rate on the formation of flow-driven confined precipitate patterns

Phys. Chem. Chem. Phys., **22**, 13390–13397 (2020), IF₂₀₂₀ = 3.676

4. E. Balog, K. Bittmann, K. Schwarzenberger, K. Eckert, A. De Wit, G. Schuszter

Influence of microscopic precipitate structures on macroscopic pattern formation in reactive flows in a confined geometry

Phys. Chem. Chem. Phys., **21**, 2910–2918 (2019), IF₂₀₁₉ = 3.43

$$\Sigma \text{IF} = 13.806$$

4.2 Other Scientific Publications

1. A. Szerlauth, E. Balog, D. Takács, Sz. Sáringér, G. Varga, G. Schuszter, I. Szilágyi

Self-assembly of delaminated layered double hydroxide nanosheets for the recovery of lamellar structure

Colloids Interface Sci. Commun., **46**, 100564 (2022), IF₂₀₂₂ = 5.633

2. K.V. Bere, E. Nez, E. Balog, L. Janovák, D. Sebők, Á. Kukovecz, C. Roux, V. Pimienta, G. Schuszter

Enhancing the yield of calcium carbonate precipitation by obstacles in laminar flow in a confined geometry

Phys. Chem. Chem. Phys., **23**, 15515–15521 (2021), IF₂₀₂₁ = 3.945

$$\Sigma \text{IF} = 9.578$$

5 Lectures

National lectures related to the dissertation: **12**

International lectures related to the dissertation: **4**

Other Lectures: **1**

5.1 Lectures Related to the Dissertation

1. E. Papp-Balog, Á. Tóth, G. Schuszter

A reakció és az anyagtranszport relatív sebességének hatása csapadékképző reakciók termékeinek mikro- és makroszerkezetére

Preliminary presentation of dissertation, Reaction Kinetics and Photochemistry Working Group of HSA, October 26–27, 2023; Mátrafüred, Hungary

2. E. Balog, G. Schuszter

Fémorganikus szilárd térhálók képződésének kinetikai vizsgálata és áramlásvezérelt szintézise vékony folyadékrétegben

Institutional ÚNKP conference, June 29, 2023; Szeged, Hungary (online)

3. E. Balog, K. Bene, Á. Tóth, G. Schuszter

Synthesis and composition modification of precipitate tubes in a confined flow reactor

Japanese–Hungarian Workshop on Reaction Kinetics, Nonlinear and Material Science, March 14, 2023; Budapest, Hungary

4. E. Balog, G. Varga, Á. Kukovecz, Á. Tóth, D. Horváth, I. Lagzi, G. Schuszter

ZIF fémorganikus térhálók különböző polimorfjainak előállítása termodinamikai és kinetikai szabályozással

Reaction Kinetics and Photochemistry Working Group of HSA, October 27–28, 2022; Mátrafüred, Hungary

5. E. Balog, P. Papp, Á. Tóth, D. Horváth, G. Schuszter

The impact of reaction rate on the formation of flow-driven confined precipitate patterns

COST Chemobrionics Pisa Annual Meeting, September 05–07, 2022; Pisa, Italy

6. E. Balog, P. Papp, Á. Tóth, D. Horváth, G. Schuszter

The impact of reaction rate on the formation of flow-driven confined precipitate patterns

Oscillations and Dynamic Instabilities in Chemical Systems (Gordon Research Seminar), July 16–17, 2022; Easton, MA, USA

7. E. Balog, P. Papp, Á. Tóth, D. Horváth, G. Schuszter

A reakciósebesség hatása a vékony folyadékrétegben kialakuló áramlásvezérelt csapadék-mintázatokra

Reaction Kinetics and Photochemistry Working Group of HSA, October 21–22, 2021;
Mátrafüred, Hungary

8. **E. Balog**, G. Varga, Á. Kukovecz, Á. Tóth, D. Horváth, I. Lagzi, G. Schuszter
A ZIF-8 fémorganikus térháló képződésének kinetikai vizsgálata és áramlásvezérelt szintézise vékony folyadékrétegben
Summer University in the Carpathian Basin, July 6–10, 2021; Budapest, Hungary (online)
9. **E. Balog**, R. Zahorán, I. Lagzi, G. Schuszter
The kinetics of zeolitic imidazolate framework (ZIF-8) formation and synthesis in confined flow reactor
2nd International Conference on Reaction Kinetics, Mechanisms and Catalysis, May 20–22, 2021; Budapest, Hungary (online)
10. **E. Balog**, R. Zahorán, P. Papp, D. Horváth, I. Lagzi, G. Schuszter
A ZIF-8 fémorganikus hálózat képződésének kinetikai vizsgálata és áramlásvezérelt szintézise vékony folyadékrétegben
Reaction Kinetics and Photochemistry Working Group of HSA, November 06, 2020; Hungary (online)
11. **E. Balog**, G. Schuszter
Áramlásvezérelt csapadékképződés vékony folyadékrétegben
Institutional ÚNKP conference, July 17, 2020; Szeged, Hungary (online)
12. **E. Balog**, G. Schuszter
Áramlásvezérelt csapadékképződés vékony folyadékrétegben
Reaction Kinetics and Photochemistry Working Group of HSA, November 07–08, 2019; Mátrafüred, Hungary
13. **E. Balog**, G. Schuszter
Áramlásvezérelt csapadékképződés vékony folyadékrétegben
XLII. Chemistry Lectures, October 28–30, 2019; Szeged, Hungary
14. **E. Balog**, G. Schuszter
Áramlásvezérelt csapadékképződés vékony folyadékrétegben
National Scientific Students' Associations Conference, March 21–23, 2019; Budapest, Hungary
15. **E. Balog**, G. Schuszter
Áramlásvezérelt csapadékképződés vékony folyadékrétegben
Scientific Students' Associations Conference, November 22, 2018; Szeged, Hungary

16. **E. Balog**, G. Schuszter

Áramlásvezérelt csapadékképződés vékony folyadékrétegben

XLI. Chemistry Lectures, October 15–17, 2018; Szeged, Hungary

5.2 Other Lectures

1. **E. Balog**, K. Bene, G. Schuszter

Kompozit fémorganikus hálózatok előállítása és képződésének kinetikai vizsgálata

Institutional ÚNKP conference, June 13, 2024; Szeged, Hungary (online)

6 Posters

International Poster Presentations Related to the Dissertation: 3

6.1 Poster Presentations Related to the Dissertation

1. **E. Balog**, P. Papp, Á. Tóth, D. Horváth, G. Schuszter

The impact of reaction rate on the formation of flow-driven confined precipitate patterns

COST Chemobrionics Pisa Annual Meeting, September 05–07, 2022; Pisa, Italy

2. **E. Balog**, P. Papp, Á. Tóth, D. Horváth, G. Schuszter

The impact of reaction rate on the formation of flow-driven confined precipitate patterns

Oscillations and Dynamic Instabilities in Chemical Systems (Gordon Research Conference), July 17–22, 2022; Easton, MA, USA

3. **E. Balog**, P. Papp, Á. Tóth, D. Horváth, G. Schuszter

The impact of reaction rate on the formation of flow-driven confined precipitate patterns

Oscillations and Dynamic Instabilities in Chemical Systems (Gordon Research Seminar), July 16–17, 2022; Easton, MA, USA

MTMT identification number: 10074154